

## Magnetic and structural phase transitions in Heusler type alloys $\text{Ni}_2\text{MnGa}_{1-x}\text{In}_x$

This article has been downloaded from IOPscience. Please scroll down to see the full text article.

2004 J. Phys.: Condens. Matter 16 5259

(<http://iopscience.iop.org/0953-8984/16/29/017>)

View [the table of contents for this issue](#), or go to the [journal homepage](#) for more

Download details:

IP Address: 129.252.86.83

The article was downloaded on 27/05/2010 at 16:09

Please note that [terms and conditions apply](#).

# Magnetic and structural phase transitions in Heusler type alloys $\text{Ni}_2\text{MnGa}_{1-x}\text{In}_x$

Mahmud Khan, Igor Dubenko, Shane Stadler and Naushad Ali<sup>1</sup>

Department of Physics, Southern Illinois University, Carbondale, IL 62901, USA

Received 2 March 2004

Published 9 July 2004

Online at [stacks.iop.org/JPhysCM/16/5259](http://stacks.iop.org/JPhysCM/16/5259)

doi:10.1088/0953-8984/16/29/017

## Abstract

X-ray diffraction, magnetization, electrical resistivity and thermal expansion measurements were done on a series of Heusler alloys of the form  $\text{Ni}_2\text{MnGa}_{1-x}\text{In}_x$   $0 < x < 0.25$ . X-ray diffraction patterns indicate that the samples possess a highly ordered Heusler alloy  $L2_1$  type structure. Due to the larger radii of the In ion, the lattice parameters were found to expand with increasing In concentration. The negative volume anomaly ( $\sim -0.1\%$ ) is found to accompany the martensitic transition. With increasing In content, a linear decrease of the martensitic transition and the Curie temperatures were observed. The compositional–transition temperature phase diagram is evaluated. Possible reasons for the structural transformations are discussed.

## 1. Introduction

The Heusler alloys that undergo a martensitic transformation from a highly symmetric cubic austenitic to a low symmetry martensitic phase are of particular interest due to their unusual thermoelastic properties. A superelasticity of a few per cent, and thermally recoverable strains as large as 20% are observed in these materials [1]. Materials exhibiting these phenomena are called ‘shape-memory’ materials for their ability to reverse large stress-induced structural deformations, and hence they are important for many engineering applications, such as in robotics, that require the development of actuator materials having large strains, appreciable thrust and rapid response time.

$\text{Ni}_2\text{MnGa}$ , a manganese based Heusler alloy, undergoes a martensitic transformation upon cooling along with a ferromagnetic alignment of the 3d magnetic moments. The ferromagnetism in this alloy results from the indirect exchange interaction between the magnetic ions, usually described in terms of the local magnetic moment at the Mn site [2, 3]. Due to the magnetically ordered martensitic phase, this alloy has gained intense interest from a scientific point of view, and also due its potential application in building a new class of actuator

<sup>1</sup> Author to whom any correspondence should be addressed.

materials in which the shape memory properties can be controlled by application of magnetic fields [4].

In stoichiometric  $\text{Ni}_2\text{MnGa}$  that has an  $L2_1$  crystal structure at room temperature, a first order martensitic structural transition, from the parent cubic (austenitic) phase to a low temperature (LT) complex tetragonal structure, takes place at  $T_M = 202$  K, and ferromagnetic order sets in at  $T_C = 376$  K [5]. The step-like variation of the magnetization, magnetic susceptibility, magnetostriction and resistivity has been observed in this system at the martensitic transition [6, 7]. Positive and negative volume anomalies were also found to accompany the transitions from ferromagnetic austenitic and paramagnetic austenitic to martensitic phases, respectively [8]. The values of  $T_M$  and  $T_C$  vary significantly with the chemical composition. The partial substitution of Mn with Ni results in an increase of  $T_M$  and a decrease of  $T_C$  and, at some critical concentration,  $T_M$  and  $T_C$  coincide [3]. On the other hand, substituting Mn with Fe results in a decrease of  $T_M$  and an increase of  $T_C$  [9]. The increase of  $T_C$  with increasing pressure was found in Mn containing Heusler alloys from hydrostatic pressure experiments [10].

It was conjectured that the Heusler structure is stabilized because the Fermi surface barely touches the (110) Brillouin-zone boundary [5]. Recently it was suggested that a band Jahn–Teller effect accompanies the martensitic transformation and the model was confirmed by polarized neutron scattering experiments, where the transfer of magnetic moment from Mn to Ni was found in the martensitic phase [11, 12]. Thus the magnetic and structural properties of  $\text{Ni}_2\text{MnGa}$  are strongly dependent on internal parameters such as interatomic distances, stoichiometry, density of 3d electron states, concentration of conduction electrons and d–d exchange interaction [6].

Although it has been a subject of interest over the last few years, many aspects of the behaviours of  $\text{Ni}_2\text{MnGa}$  are not clearly understood. The relative contributions of internal parameters to property variations of  $\text{Ni}_2\text{MnGa}$  based alloys are not sufficiently clarified. Because of the band character of the magnetism, the magnetic characteristics of Heusler alloys are determined by the density of d-states at the Fermi level and the exchange splitting parameter, and depend on the structure and composition. Therefore, in most cases of the Ni or Mn subsystem doped alloys, several parameters are varied.

This work was undertaken to study the structural, magnetic and electrical properties of the  $\text{Ni}_2\text{MnGa}$  system by the substitution of Ga by isoelectronic In. The system has been studied with respect to temperature and composition by magnetization, resistivity and thermal expansion measurements.

## 2. Experimental procedure

5–7 g of stoichiometric polycrystalline ingots of  $\text{Ni}_2\text{MnGa}_{1-x}\text{In}_x$  ( $0.0 \leq x \leq 0.25$ ) were prepared by conventional arc melting in an argon atmosphere using high purity Ni, Mn, Ga and In. The weight loss after melting was found to be less than 0.3%. For homogenization, the samples were annealed in vacuum for 72 h at 900 °C, and slowly cooled down to room temperature. In order to measure the electrical resistivity, thermal expansion and magnetic properties, samples of different shapes were cut with a diamond blade from the homogenized ingots.

X-ray diffraction measurements were conducted at room temperature for phase identification and lattice constant determination. The measurements were done on a GBC MMA (Mini Materials Analyzer) x-ray diffractometer that used Cu  $K\alpha$  radiation and Bragg–Brentano geometry. Small pieces of the samples were crushed to powder form by hand tools without maintaining any particular grain size, and were used for XRD measurements.

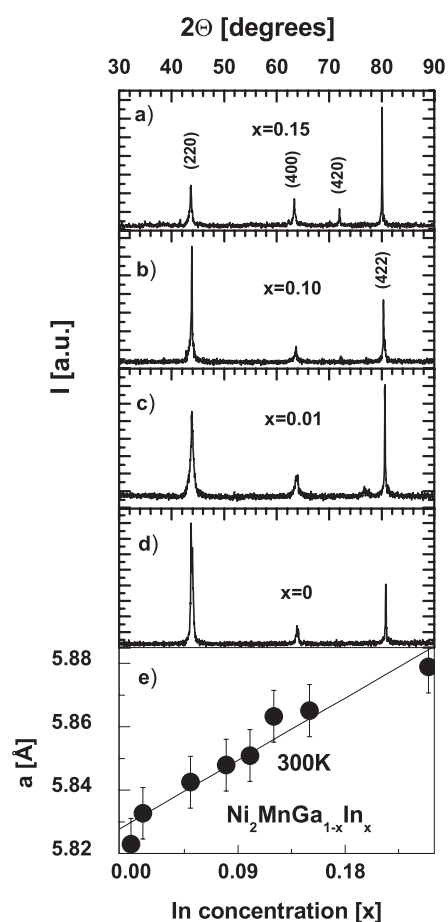


**Figure 1.** X-ray powder diffraction patterns of  $\text{Ni}_2\text{MnGa}_{1-x}\text{In}_x$  system with  $x =$  (a) 0.15, (b) 0.10, (c) 0.01, (d) 0.00, and (e) cell parameter variation with respect to In concentration ( $x$ ) at room temperature.

The magnetization measurements were performed on a superconducting quantum interference device (SQUID) made by Quantum Design Inc. The measurements were performed in a temperature range of 5–400 K and a magnetic field of up to 55 kOe. Direct current resistivity, using the four-probe method, was measured over the same temperature range as the magnetization measurements. To eliminate the contribution of thermoelectric effects, the current direction was reversed and an average of the voltage drops in each direction was taken. Thermal expansion was measured using the high-resolution capacitance dilatometry method in the temperature range 80–295 K [13].

### 3. Experimental results and discussion

Figure 1(a–d) shows typical powder x-ray diffraction patterns at room temperature of the  $\text{Ni}_2\text{MnGa}_{1-x}\text{In}_x$  system. The crystal structures at room temperature are found to be the cubic Heusler  $L2_1$  type. Due to the larger In radius, with increasing indium concentration, an apparent linear increase in the lattice constants is observed (see inset of figure 1(e)).

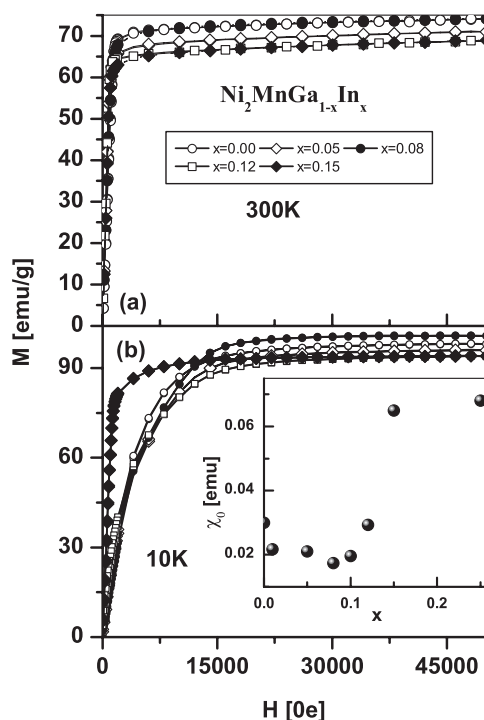


**Figure 2.** Magnetization curves  $M(H)$  of the  $\text{Ni}_2\text{MnGa}_{1-x}\text{In}_x$  at (a) 300 K and (b) 10 K. The inset shows the low field susceptibility  $\chi_0$  versus In concentration of the  $\text{Ni}_2\text{MnGa}_{1-x}\text{In}_x$  system at 10 K.

The magnetization curves of the system at 10 and 300 K are presented in figures 2(a) and (b), respectively. All compounds are found to exhibit ferromagnetic behaviour with saturation magnetizations ( $M_0$ ) of approximately 98 and 72  $\text{emu g}^{-1}$  at 10 and 300 K, respectively. At 300 K all the samples are observed to possess a typical ‘soft’ ferromagnetic behaviour of magnetization characterized by low saturation fields, whereas at 10 K only the alloys with concentration  $x \geq 0.14$  exhibit this behaviour. The alloys with  $x < 0.14$  possess ‘hard’ ferromagnetic properties at 10 K. This abrupt increase of saturation field indicates an increase of magnetic anisotropy in the compounds with concentration  $x < 0.14$ . The transformation from ‘hard’ to ‘soft’ ferromagnetic type can be clearly seen from step-like increases of the low field susceptibility  $\chi_0$  of the  $\text{Ni}_2\text{MnGa}_{1-x}\text{In}_x$  system at  $x \geq 0.14$  (see inset of figure 2). The martensitic transformation is accompanied by an increase of the magnetic anisotropy and a reduction in the number of easy axes due to a crystal structure transition from cubic (austenite state) to tetragonal phases (martensitic state). Thus, the  $\text{Ni}_2\text{MnGa}_{1-x}\text{In}_x$  samples at low temperature in the concentration range  $x < 0.14$  are in the martensitic state while the compounds with  $x \geq 0.14$  remain in the austenite state at low temperature.

Magnetization versus temperature curves of  $\text{Ni}_2\text{MnGa}_{1-x}\text{In}_x$  at  $H = 1000$  Oe are presented in figure 3. With decreasing temperature in the high temperature region ( $T > 350$  K) the magnetization of all the alloys increases sharply, indicating a ferromagnetic–paramagnetic transition at  $T_C$ . Taking into consideration that the structural change at  $T_M$  of these alloys is accompanied by a drastic decrease in magnetization [6, 7], we observe the martensitic transition in alloys with composition  $x < 0.14$  (see figure 3), and the transition is no longer observed in alloys with composition  $x \geq 0.14$ . The alloys with composition  $x < 0.14$  are also found to

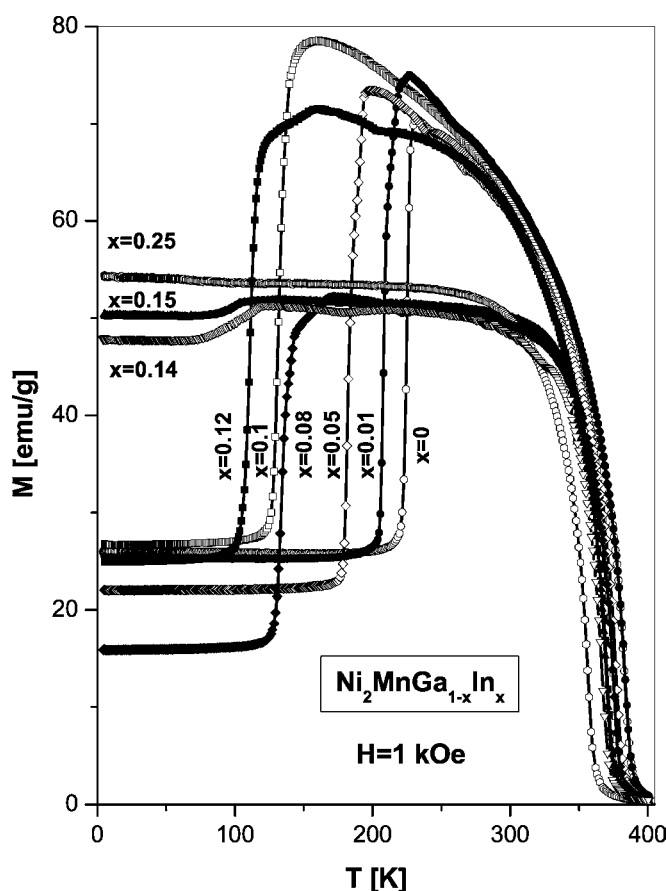


**Figure 3.** The temperature variation of magnetization  $M(T)$  of  $\text{Ni}_2\text{MnGa}_{1-x}\text{In}_x$  obtained at a magnetic field of 1 kOe.

exhibit pre-martensitic transitions [14, 15] above  $T_M$ . As shown in figure 4, the resistivity curves of the alloys in the concentration range  $0 < x < 0.15$  possess a pronounced sharp variation at  $T_M$ . The change in slope of the resistivity curves at  $T_C$  is due to the reduction of electron scattering on magnetic fluctuation. The thermal expansion of  $\text{Ni}_2\text{MnGa}_{1-x}\text{In}_x$  compounds with  $0 < x < 0.15$  exhibits a step like negative volume anomaly,  $\Delta V/V \cong 3\Delta l/l \sim -0.1\%$ , at  $T_M$  (see inset of figure 4). It is interesting to note that the value of the negative volume anomaly decreases with increasing In concentration. Such step like variation of the thermal expansion and resistivity are typical for first-order transitions.

The variation of the phase transition temperatures with respect to In concentration evaluated from our results is shown in the  $(T-x)$ -phase diagram (figure 5). The pre-martensitic anomalies of  $M(T)$  at  $T_P$  are shown in the inset of figure 5. Increasing In content results in a linear decrease of all phase transition temperatures  $T_C$ ,  $T_P$  and  $T_M$ . The slope of  $T_M$  is larger than that of  $T_C$ .

Since In and Ga are isoelectronic, substitution of Ga with In is not expected to change the net conduction electron density. Therefore the decrease in  $T_M$  and  $T_C$  cannot be explained in terms of conduction electron density. However, due to the larger ionic radius of In, there is an increase in the cell volume of the system that results in an increase in the distances between

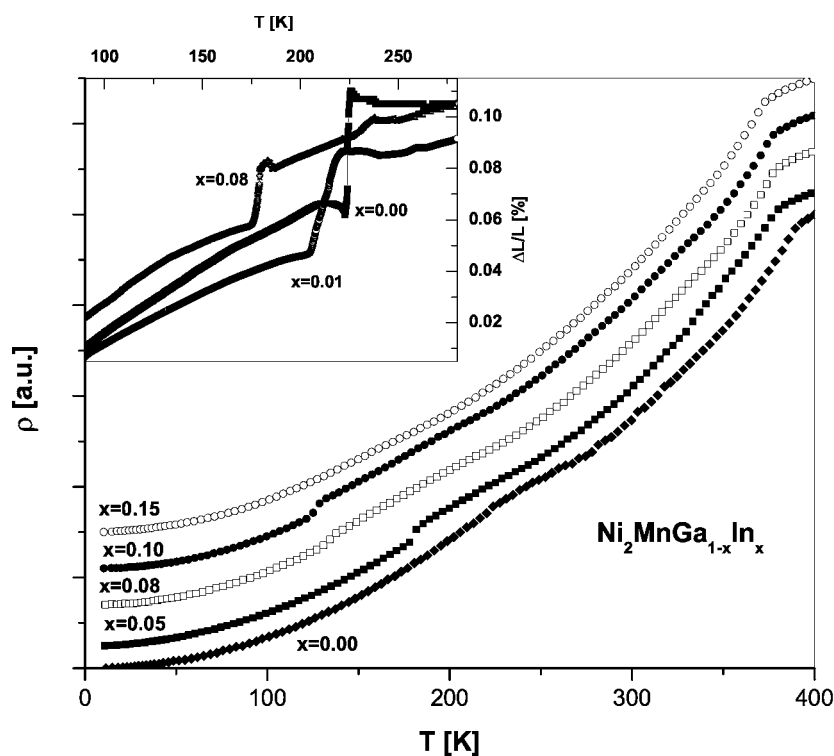


**Figure 4.** Resistivity  $\rho(T)$ , and thermal expansion (inset) as a function of temperature of  $\text{Ni}_2\text{MnGa}_{1-x}\text{In}_x$ .

the Mn atoms. A linear increase of  $T_C$  and decrease of  $T_M$  with increasing hydrostatic pressure were found for  $\text{Ni}_2\text{MnGa}$  [10]. Hence the effect of changing distances between Mn atoms on the Curie temperature is clear.

It was shown that the application of hydrostatic pressure on  $\text{Ni}_2\text{MnGa}$  results in a decrease of the Mn–Mn distance, and thus causes a decrease of  $T_M$  [10]. In our case, In substitution of the Ga site results in an increase of the Mn–Mn distance and also causes a decrease of  $T_M$ . From the band calculations [1], the free energy of the martensitic phase was found to have a dependence on the cell parameters  $c/a$  ratio. Based on this calculation and our observation, it is natural to propose that the expansion of the volume of the unit-cell austenitic phase results in a loss of the martensitic phase stability because of the shift of the  $c/a$  ratio from its optimum value. Thus there is a range of unit-cell volume for which the martensitic transformation can be observed in Heusler systems. In the case of  $\text{Ni}_2\text{MnGa}_{1-x}\text{In}_x$  compounds, the austenitic phase stabilizes and no martensitic transition is observed for  $a > 5.86 \text{ \AA}$ .

For samples with  $x = 0.14$  and  $0.15$ , small anomalies are observed in the magnetization versus temperature curves at 100 and 95 K, respectively. The nature of these anomalies is not clearly understood from the obtained results as they only appear on the magnetization versus temperature curves and not on the resistivity curves. The coexistence of cubic and tetragonal phases at low temperature was found in cubic  $\text{YMn}_2$  [16]. In this compound a first order transition takes place on lowering the temperature, and during this transition a small portion of the parent cubic phase remains unchanged while the major portion undergoes a tetragonal phase transition. In the light of this information, it is possible that the anomalies observed in the

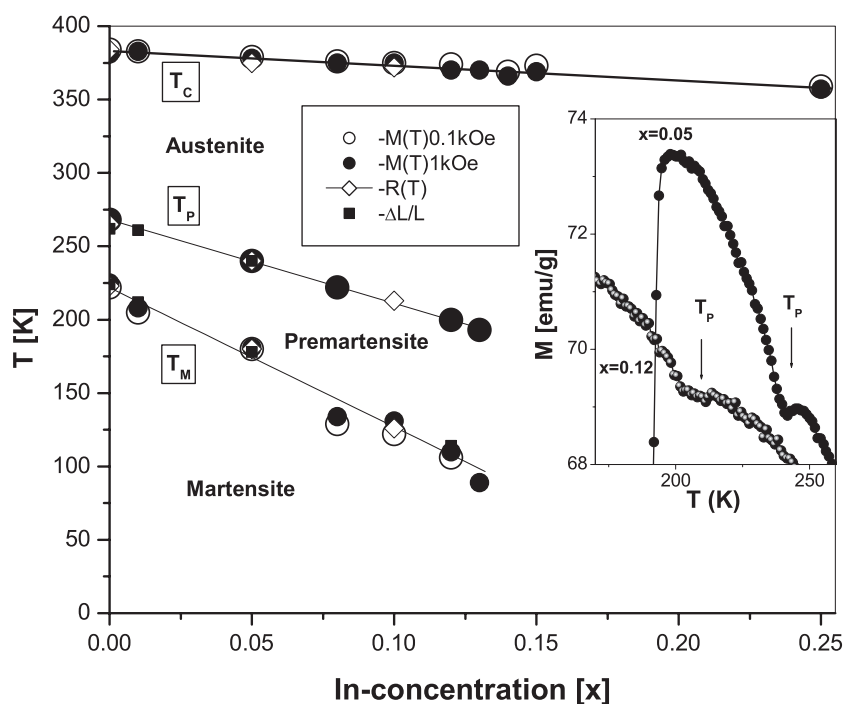


**Figure 5.**  $(T-x)$ -phase diagram of  $\text{Ni}_2\text{MnGa}_{1-x}\text{In}_x$  obtained from  $M(T)$ ,  $\rho(T)$ , and thermal expansion measurements. The inset shows the pre-martensitic anomaly of  $M(T)$ .

magnetization versus temperature curves for  $\text{Ni}_2\text{MnGa}_{1-x}\text{In}_x$  samples with  $x = 0.14$  and  $0.15$  are due to the fact that at low temperature a small amount of martensitic phase coexists with the parent cubic phase. Based on the obtained results no conclusion can be made regarding these anomalies and further experimental studies are needed. Therefore the study of these anomalies would be a subject for further studies.

#### 4. Conclusion

The results of these experimental studies establish the general tendency of both martensitic transition temperature  $T_M$  and Curie temperature  $T_C$  to decrease with increasing In concentration in  $\text{Ni}_2\text{MnGa}_{1-x}\text{In}_x$ . The martensitic transition has been shown to exist for alloys with  $0 < x < 0.14$ . For alloys with  $x \geq 0.14$  no clear martensitic transitions are observed in our experimental data, and the alloys are apparently still in the austenite phase at low temperature. This could be due to the coexistence of multiple phases in the alloys with  $x \geq 0.14$ . The decrease of  $T_M$  is a possible consequence of the change of relative position of the Brillouin zone boundary and the Fermi surfaces which is caused by the increase of the unit cell volume. The reason for the drop of the Curie temperature with increasing In concentration is a result of the increase in Mn–Mn inter-atomic distance.

#### Acknowledgment

This work was supported by the Consortium for Advanced Radiation Sources, University of Chicago.



## References

- [1] Ayuela A, Enkovaara J, Ullakko K and Nieminen R M 1999 *J. Phys.: Condens. Matter* **11** 2017
- [2] Plogmann S, Schlathöler T, Braun J, Neumann M, Yarmoshenko Yu M, Yablonskikh M V, Shreder E I, Kurmaev E Z, Wrona A and Slebarski A 1999 *Phys. Rev. B* **60** 6428
- [3] Kubler J, Williams A R and Sommers C C 1983 *Phys. Rev. B* **28** 1745
- [4] Ullakko K, Huang J K, Kantner C, O'Handley R C and Kokorin V V 1996 *Appl. Phys. Lett.* **69** 1966
- [5] Webster P J, Ziebeck K R A, Town S L and Peak M S 1984 *Phil. Mag.* **B 49** 295
- [6] Vasil'ev A N, Bozhko A D, Khovailo V V, Dikshtein I E, Shavrov V G, Buchelnikov V D, Matsumoto M, Suzuki S, Takagi T and Tani J 1999 *Phys. Rev. B* **59** 1113
- [7] Matsumoto M, Takagi T, Tani J, Kanomata T, Muramatsu N and Vasil'ev A N 1999 *Mater. Sci. Eng. A* **273–275** 326
- [8] Vasil'ev A N, Estrin E I, Khovailo V V, Bozhko A D, Ischuk R A, Matsumoto M, Takagi T and Tani J 2000 *Int. J. Appl. Electromagn. Mech.* **12** 35
- [9] Liu Z H, Zhang M, Wang W Q, Wang W H, Chen J L, Wu G H, Meng F B, Liu H Y, Liu B D, Qu J P and Li Y X 2002 *J. Appl. Phys.* **92** 5006
- [10] Kanomata T, Shirakawa K and Kaneko T 1987 *J. Magn. Magn. Mater.* **65** 76
- [11] Khovailo V V, Takagi T, Tani J, Levitin R Z, Cherechukin A A, Matsumoto M and Note R 2002 *Phys. Rev. B* **65** 092410
- [12] Brown P J, Bargawi A Y, Crangle J, Neumann K-U and Ziebeck K R A 1999 *J. Phys.: Condens. Matter* **11** 4715
- [13] Steinitz M O, Genossar J, Schnepfand W and Tindall D A 1986 *Rev. Sci. Instrum.* **57** 297
- [14] Planes A, Obrado E, Gonzalez-Comas A and Manosa L 1997 *Phys. Rev. Lett.* **79** 3926
- [15] Zuo F, Su X and Wu K H 1998 *Phys. Rev. B* **58** 11127
- [16] Gaidukova I Yu and Markosyan A S 1982 *Phys. Met. Metallogr.* **54** 168